

**Comparative study of anharmonicity: Ni(111), Cu(111), and Ag(111)**Ahlam N. Al-Rawi,<sup>1</sup> Abdelkader Kara,<sup>1</sup> and Talat S. Rahman<sup>1,2</sup><sup>1</sup>*Department of Physics, Cardwell Hall, Kansas State University, Manhattan, Kansas 66506*<sup>2</sup>*Fritz-Haber-Institut der Max-Planck-Gesellschaft, Faradayweg 4-6, D14195 Berlin, Germany*

(Received 29 May 2002; revised manuscript received 21 August 2002; published 31 October 2002)

We present a comparative study of the structure and the dynamics of the most close packed surface of Ni, Cu, and Ag from near room temperature up to  $0.9T_m$ , using molecular dynamics simulations and interaction potentials from the embedded atom method. Calculated shifts in the surface phonon frequencies, the broadening of their linewidths, and the variations in the mean square vibrational amplitudes of surface atoms, as a function of temperature, indicate that anharmonic effects are small on these surfaces. The surface thermal expansion of these three (111) surfaces is also found to be smaller than that of the respective (100) and (110) surfaces. Additionally, we do not find any premelting or pronounced disordering on these surfaces, in the temperature range considered.

DOI: 10.1103/PhysRevB.66.165439

PACS number(s): 68.35.Ja, 68.35.Md

**I. INTRODUCTION**

Several unresolved questions foster continued interest in understanding how anharmonic effects at surfaces differ from those in the bulk solid. The reduced coordination of the surface atoms, as compared to their bulk counterparts, impacts the surface electronic charge distribution and consequently the nature of the interatomic potential experienced by the surface atoms. As manifestations of these changes, surface atoms may display equilibrium positions, even at low temperatures, which are different from those in the bulk. This can be seen from the survey of experimental surface structure data<sup>1</sup> in which surfaces are found to undergo “relaxation” (i.e., a deviation from the bulk value for the top interlayer separations), or “reconstruction” (i.e., a lateral rearrangement of the top layer atoms). Analysis of the data from a large set of metal surfaces shows a link between the surface geometry and the deviation from bulklike behavior,<sup>2</sup> the effect being more pronounced the more open the surface. With increasing temperature, thermal expansion, atomic vibrational amplitudes, and phonon-phonon interactions induced by anharmonic contributions to the interaction potentials may also affect the bulk and the surface atoms differently. For example, it may cause the surface to disorder, roughen, or melt before the bulk. Indeed, experimental and theoretical work on the (110) surface of the three metals of interest here—Ni,<sup>3,4</sup> Cu,<sup>5–8</sup> and Ag (Refs. 9 and 10)—display anomalous thermal behavior. By the same token, the thermal behavior of the close-packed, (111), surface of the same metals was generally assumed to be almost bulklike until a few years ago, when medium-energy ion-scattering (MEIS) data became available. The conclusions from the MEIS measurements are that (1) anomalous thermal expansion begins on Ag(111) at 670K and reaches a value 10% above that in the bulk at 1150K (Ref. 11); (2) anomalous behavior on Cu(111) is somewhat delayed and smaller,<sup>12</sup> with maximum thermal expansion of 4.3% at 1180 K; and (3) Ni(111) exhibits an almost bulklike thermal expansion from 300 to 1100 K.<sup>13</sup> In each case, the mean square vibrational amplitudes of the surface atoms are correspondingly enhanced. These results point to the material specificity of surface thermal expansion and surface atomic vibrational amplitudes: Ag(111) displaying

the greatest enhancement of surface anharmonicity, followed by Cu(111), and Ni(111) behaving in a bulklike manner. More importantly, the close-packed (111) surface appears to be as vulnerable to anharmonic effects (which tend to lead to surface disordering, roughening, and melting) as its more open counterpart, the (110) surface. It is thus a surprise that there is a lack of other observations supporting this claim. Is it then that the (111) surfaces of Ag and Cu are indeed more affected by anharmonicity than their bulk? If so, why is the thermal behavior of Ni(111) different from that of the other two?

To address the issue of anomalous surface thermal expansion on Ag(111) we recently carried out a molecular dynamics study using empirical but reliable many-body interaction potentials.<sup>14</sup> In the temperature range 300–1100 K we do not find the surface thermal expansion to be different from that in the bulk. Through calculations of the temperature dependencies of the atomic vibrational amplitudes, surface phonon frequencies and their linewidths, Grüneisen parameters, and anharmonic constants, we have provided further measures of the extent of surface anharmonicity on Ag(111).

In the present paper our goal is to compare anharmonicity on Ag(111), Cu(111), and Ni(111), using classical molecular dynamics simulations and interaction potentials from the embedded atom method (EAM).<sup>15</sup> For this purpose, we calculate characteristics of systems that are reflective of anharmonic effects. While surface thermal expansion and atomic vibrational amplitudes are obvious candidates for the exhibition of anharmonic effects, phonon frequencies and their line broadening are also expected to change with temperature, because of phonon-phonon interactions introduced by anharmonicity. Note that since we extract our results from molecular dynamics simulations, anharmonic terms in the interaction potential are included in an exact manner. Together with the work on Al(111) by Zivieri *et al.*,<sup>16</sup> the present study provides a good overview of anharmonic effects on fcc(111) surfaces. Further, by comparing results on fcc(111) surfaces to the corresponding (110) surfaces, we provide a measure of the differences in the anharmonic behavior of a close-packed surface of the same metal to that of one of its “open” surfaces. In Sec. II we provide some details of the calculations of the surface structural and dynamical proper-

ties. Each subsection contains the results and the discussion of the particular quantity calculated. The study concludes with a summary of the overall findings.

## II. CALCULATION OF SURFACE DYNAMICS AND STRUCTURE

We employ standard molecular dynamics techniques to simulate the positions and velocities of atoms for a chosen time-period by solving numerically Newton's equations of motion using Nordsieck's algorithm.<sup>17</sup> For all calculations, a time step of 1 fs is used. The molecular dynamics (MD) cell consists of 3024 atoms divided into 18 layers for all cases. Periodic boundary conditions were imposed in the  $x$ - $y$  plane (parallel to the surface). For each temperature, and at zero pressure, we performed a constant temperature, constant pressure simulation for a bulk system, to calculate the lattice constant at that temperature. The surface cell is then constructed with the lattice constant corresponding to the temperature of interest. Under conditions of constant volume and constant temperature, this system is equilibrated to the desired temperature for 20 ps. Next the system is isolated and allowed to evolve in a much longer run of about 200 ps in which its total energy remains constant, and statistics on the positions and velocities of the atoms are recorded.

In the subsections below, we give a brief description of how a particular structural and dynamical quantity is calculated from the statistics collected in the MD simulation for Ni(111), Cu(111), and Ag(111). We begin with evaluation of the temperature dependent phonon frequencies and their linewidths analysis. This is followed by an examination of the mean square vibrational amplitudes and the interlayer separation of the top layers. We also calculate the anharmonic constant<sup>18,19</sup> and the Grüneisen parameter. Next we present results for the long and short range orderings at the surface and examine the exchange of atoms in the top layers. The temperature range of interest in these calculations is 300 K to  $0.9T_m$ . Theoretical bulk melting temperatures based on EAM potentials are 1170, 1340, and 1740 K,<sup>20</sup> for Ag, Cu, and Ni, respectively. This is only slightly less than the experimentally observed values<sup>21</sup> of 1235, 1358, and 1743 K, for Ag, Cu, and Ni, respectively.

### A. Phonon frequencies and linewidths

Surface phonon spectral densities may be calculated from the dynamic structure factor<sup>22</sup> or, in the one-phonon approxi-

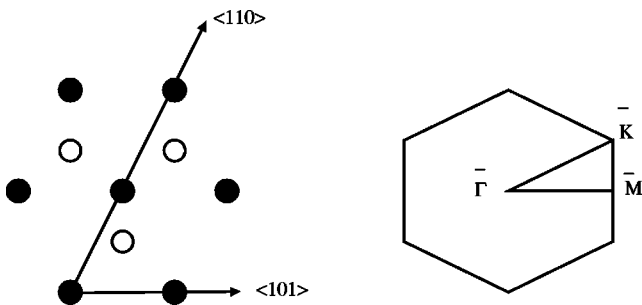


FIG. 1. The top view of the fcc(111) surface and the two dimensional Brillouin zone.

mation, from the temporal Fourier transform of the layer-averaged, displacement-displacement auto-correlation functions.<sup>23</sup> In practice, however, since the reference positions for atomic displacements are not well defined, velocities instead of displacements are used to obtain the phonon spectral densities.<sup>24,25</sup> We have

$$g_{\alpha\alpha}(\mathbf{Q}_{\parallel}, \omega) = \left| \int e^{i\omega t} \left( \sum_{j=1}^{N_l} v_{j\alpha}(t) e^{i\mathbf{Q}_{\parallel} \cdot \mathbf{R}_j^0} \right) dt \right|^2, \quad (1)$$

where  $g_{\alpha\alpha}$  is the spectral density for displacements along direction  $\alpha (=x, y, z)$  of atoms in layer  $l$ ,  $N_l$  is the number of atoms in the layer,  $\mathbf{Q}_{\parallel}$  is the two dimensional wave-vector

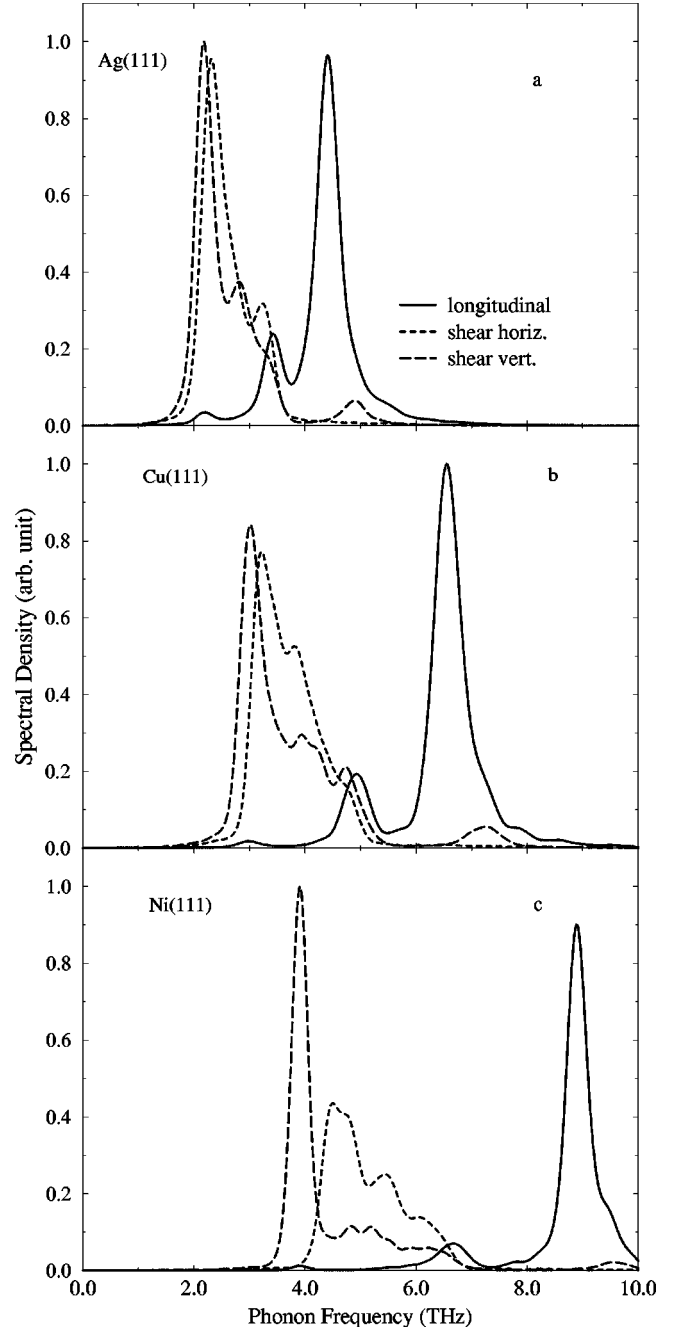


FIG. 2. Phonon spectral densities at  $\bar{M}$  at 300K for (a) Ag(111), (b) Cu(111), and (c) Ni(111).

TABLE I. Ag(111): Comparison of frequencies (in THz) of surface modes at  $\bar{M}$  with previous results. EELS stands for electron energy loss spectroscopy.

Element	Source	$L$	SV
Ag(111)	Our calculation	4.33	2.15
	First principle (Ref. 28)	4.60	2.02
	Lattice dynamics (Ref. 30)	4.37	2.10
	Lattice dynamics (Ref. 31)	4.80	2.30
	He scattering (Ref. 35)	4.23	2.10
	HTFS (Ref. 50)	-	2.20
	EELS (Ref. 51)	4.60	2.20
	Our calculation	6.51	3.02
Cu(111)	Lattice dynamics (Ref. 30)	6.58	3.16
	First principles (Refs. 28 and 33)	6.50	3.20
	Lattice dynamics (Ref. 32)	-	3.02
	Lattice dynamics (Ref. 31)	6.70	3.20
	HTFS (Ref. 50)	-	3.16
	EELS (Refs. 36 and 52)	-	3.17
Ni(111)	Our calculation	8.88	3.91
	Lattice dynamics (Ref. 30)	8.00	3.83
	EELS (Ref. 34)	8.79	4.01

parallel to the surface, and  $\mathbf{R}_j^0$  is the equilibrium position of atom  $j$  whose velocity is  $\vec{v}_j$ . A detailed explanation of the calculation can be found elsewhere.<sup>14</sup> Figure 1 shows the geometry of the fcc(111) surface and the two-dimensional Brillouin zone. In Figs. 2(a)–2(c), we present the surface phonon frequencies at 300 K, for the modes at the  $\bar{M}$  point of the two dimensional Brillouin zone. This figure provides a good basis for comparison with results from other calculations, which are based on the harmonic approximation of lattice dynamics, and from a variety of experimental measurements that are often taken around this temperature. Table I illustrates this comparison for Ag(111), Cu(111), and Ni(111), respectively, for the shear vertical and longitudinal modes which are polarized along the surface normal and the surface plane, respectively. We have not included the shear horizontal mode in the Table as there is very little information on this mode because of inherent difficulties (selection

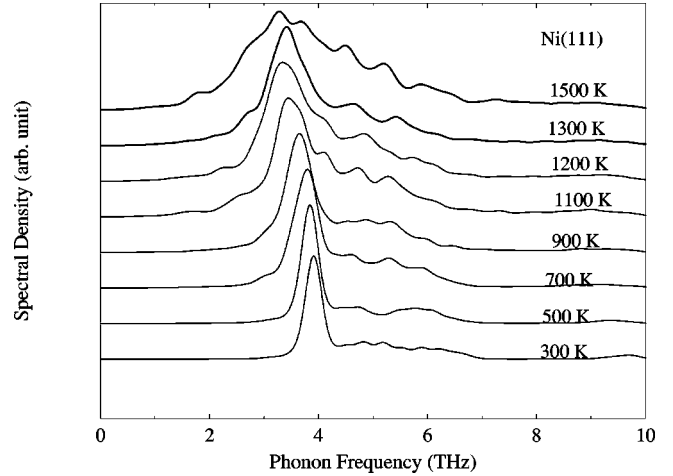


FIG. 3. Temperature variation of phonon spectral densities at  $\bar{M}$  for Ni(111).

rule violation) in measuring it by standard techniques. Our results are in good agreement with previous theoretical<sup>26–33</sup> and experimental<sup>28,33–36</sup> values. This reflects the fact that at room temperature, one would expect very small anharmonic effects. As the temperature is increased, shifts as well as broadening of the modes are expected.

Figure 3 show the temperature dependence of the spectral density for the shear vertical mode for Ni(111), at  $\bar{M}$  [the same figure for Ag(111) can be found in a previous work<sup>14</sup>]. Similar results have been obtained for Cu(111). In each case, there is clearly a shift in the frequency of this mode with increasing temperature. These shifts are given in Table II together with those for the longitudinal mode. We note that at  $\bar{M}$ , between room temperature and  $0.89T_m$ , the frequency of the shear vertical mode softens by 0.66, 0.53, and 0.63 THz for Ag(111), Cu(111), and Ni(111), respectively, while the corresponding softening for the longitudinal mode is 0.60 THz for Ag(111), 0.28 THz for Cu(111), and 0.76 THz for Ni(111). There is thus no discernible pattern in the shifts in the frequencies of these modes on the three fcc(111) surfaces, except that there is a softening in each case with increasing temperature. To our knowledge, calculations or experimental measurements are not available for phonons at high temperature for these systems. For the same temperature range, the broadening in the linewidths of the modes at

TABLE II. Surface phonon frequencies (in THz) at  $\bar{M}$ , as a function of temperature.

Element	$T(K)$	300	500	700	900	1000	1050	1100	1200	1300	1500
Ag(111)	$L$	4.33	4.16	4.13	4.00	4.10	3.73				
	SV	2.15	2.08	2.02	1.96	2.08	1.49				
Cu(111)	$L$	6.51	-	6.23	6.30	-	-	6.15	6.23		
	SV	3.02	-	2.77	2.76	-	-	2.57	2.49		
Ni(111)	$L$	8.88	8.48	8.55	8.10	-	-	8.20	8.19	8.04	8.12
	SV	3.91	3.84	3.77	3.65	-	-	3.42	3.45	3.40	3.28

TABLE III. Surface phonon linewidth (in THz) at  $\bar{M}$ , as a function of temperature.

Element	$T(K)$	300	500	700	900	1000	1050	1100	1200	1300	1500
Ag(111)	$L$	0.40	0.64	0.52	1.13	1.46	1.80				
	SV	0.22	0.42	0.64	1.12	0.90	1.10				
Cu(111)	$L$	0.14	-	0.32	0.68	-	-	0.68	0.67		
	SV	0.29	-	0.54	0.52	-	-	1.20	1.52		
Ni(111)	$L$	0.18	0.35	0.58	0.73	-	-	1.14	1.16	1.35	2.21
	SV	0.08	0.08	0.37	0.43	-	-	0.60	0.96	0.63	1.92

$\bar{M}$  with increasing temperature, for the three metal surfaces, are compiled in Table III. The determination of the broadening of the vibrational modes is a very complicated task at elevated temperatures. Indeed, when the temperature is higher than  $0.8T_m$ , there are appearances of new modes due to phonon-phonon interactions, which make the analysis challenging. Note that in Table III there is a sudden large increase in the broadening at about 800, 1000, and 1400 K for Ag, Cu, and Ni, respectively.

### B. Mean square vibrational amplitudes

The atomic mean square vibrational amplitudes are calculated using the equation

$$\langle u_{i\alpha}^2 \rangle = \frac{1}{N_l} \sum_{i=1}^{N_l} \langle [r_{i\alpha}(t) - r_{i\alpha}(0)]^2 \rangle \quad (2)$$

where  $N_l$  is the number of atoms in layer  $l$ ,  $r_i(0)$  is the initial position of atom  $i$  in layer  $l$ ,  $\langle --- \rangle$  represents an average over time, and  $\alpha$  is a Cartesian component. In applying Eq. (2) to the statistics collected for the positions of the atoms as a function of time, we discard all atoms that diffuse or evaporate. The three components of the mean square vibrational amplitudes thus obtained for the atoms in the top three layers are shown in Table IV. A plot of these quantities for the atoms in the first layer in Figs. 4(a)–4(c) shows that the mean square vibrational amplitudes along the  $z$ -direction (perpendicular to the surface) are generally larger than the in-plane ( $x$  and  $y$ ) ones for all three metals, for almost the entire temperature range. In the case of Ag(111), it is interesting that the in-plane amplitudes become comparable to the normal one close to  $T_m$ . Furthermore, in contrast to Cu(111) and Ni(111), for Ag(111) even the second and third layer atoms display enhanced vibrational amplitudes in the in-

 TABLE IV. Temperature dependence of the mean square vibrational amplitudes in units of  $10^{-2} \text{ \AA}^2$  for the atoms in the first three layers.

Element	$T(K)$	$\langle u_{1x}^2 \rangle$	$\langle u_{1y}^2 \rangle$	$\langle u_{1z}^2 \rangle$	$\langle u_{2x}^2 \rangle$	$\langle u_{2y}^2 \rangle$	$\langle u_{2z}^2 \rangle$	$\langle u_{3x}^2 \rangle$	$\langle u_{3y}^2 \rangle$	$\langle u_{3z}^2 \rangle$
Ag(111)	300	1.22	1.21	1.57	1.2	1.2	1.55	0.92	0.92	1.0
	500	2.44	2.21	2.7	1.92	1.7	2.01	1.876	1.67	1.68
	700	3.59	3.56	4.25	2.86	2.89	3.07	2.67	2.67	2.67
	900	4.97	5.30	6.55	3.81	4.23	4.66	3.524	3.82	3.99
	1000	7.12	6.56	9.29	5.36	5.12	5.93	4.678	4.64	5.0
	1050	8.14	7.51	9.26	6.25	5.65	6.56	5.534	5.07	5.46
	1100	11.2	9.06	10.57	8.86	6.64	8.05	7.64	5.86	5.86
Cu(111)	300	0.96	0.965	1.47	0.82	0.82	1.11	0.78	0.77	0.96
	700	2.73	2.85	3.64	2.27	2.20	2.63	2.12	2.19	2.33
	900	3.94	3.85	4.88	3.24	3.16	3.54	2.99	2.89	3.08
	1100	5.53	5.71	7.17	4.40	4.55	5.23	3.99	4.17	4.49
	1200	6.75	6.77	8.89	5.31	5.352	6.57	4.81	4.81	5.57
Ni(111)	300	0.55	0.58	0.94	0.47	0.49	0.65	0.44	0.46	0.58
	500	1.00	1.08	1.55	0.84	0.91	1.08	0.80	0.84	0.94
	700	1.58	1.49	2.33	1.33	1.25	1.61	1.25	1.17	1.40
	900	2.15	2.16	3.15	1.77	1.79	2.11	1.65	1.67	1.81
	1100	2.90	2.91	4.31	2.35	2.38	2.93	2.19	2.18	2.46
	1200	3.30	3.50	4.78	2.70	2.93	3.23	2.47	2.70	2.74
	1300	3.80	3.69	5.43	3.10	2.98	3.66	2.79	2.75	3.10
1500	5.37	5.11	7.31	4.35	4.08	4.98	3.92	3.64	4.11	

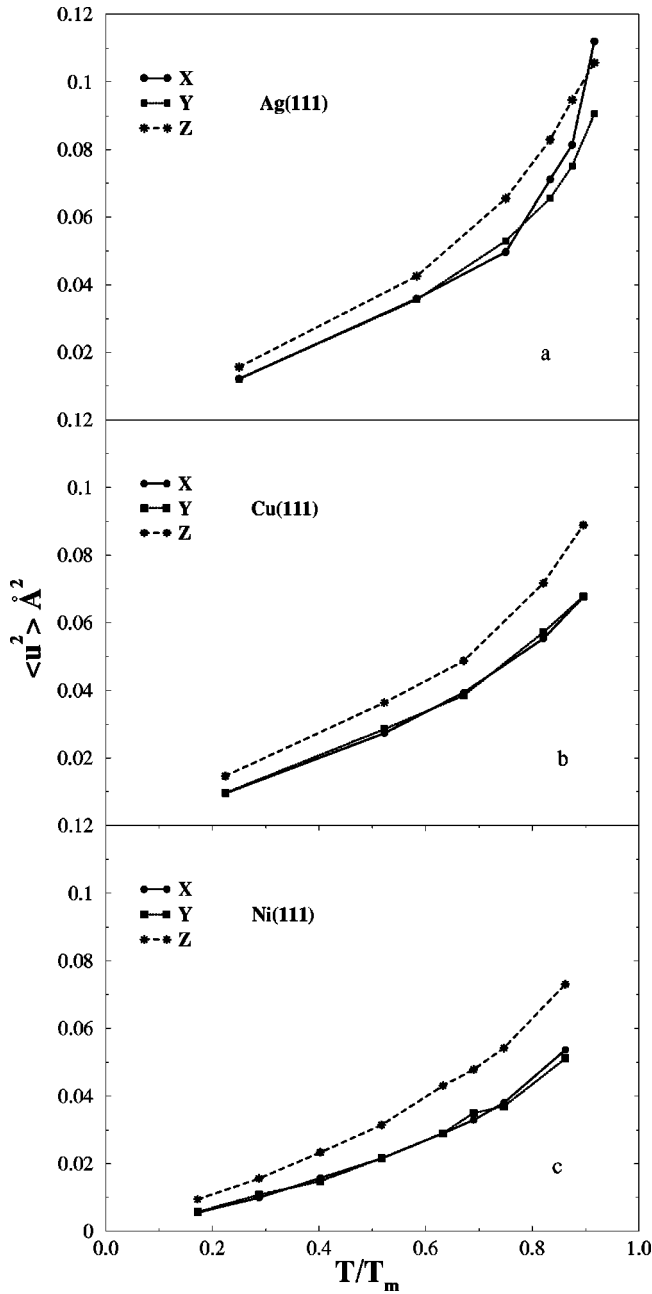


FIG. 4. Mean square vibrational amplitudes vs temperature for atoms in the top layer for (a) Ag(111), (b) Cu(111), and (c) Ni(111).

plane component. From these three figures we can conclude that, except for Ag(111) (Ref. 14) near the melting temperature, the normal component of the mean square vibrational amplitudes is larger than the in-plane components, and this difference decreases as we go deeper into the crystal, in agreement with previous work on Al(111).<sup>16</sup> A comparison of the calculated surface mean square vibrational amplitudes of Ag(111) with those of Ag(110), (Ref. 37) is shown in Fig. 5. This figure shows that the three component of the mean square vibrational amplitudes for Ag(111) and Ag(110) are about the same up to around 700 K. Beyond this temperature, for Ag(110) both the  $x$  and  $y$  components of the mean square vibrational amplitudes increase remarkably with in-

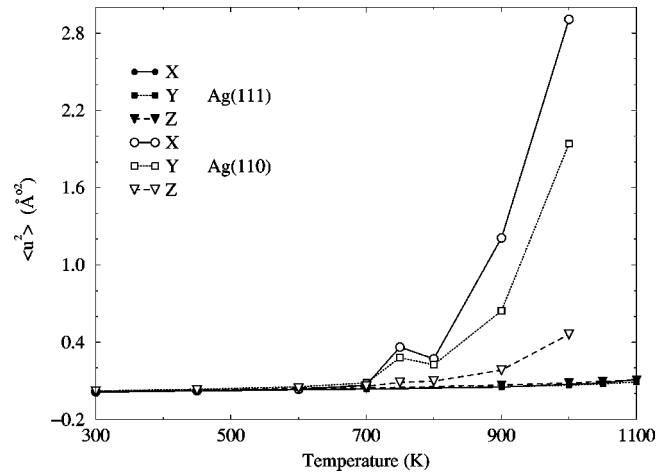


FIG. 5. Surface mean square vibrational amplitudes versus temperature for Ag(111) and Ag(110).

creasing temperature, but the  $x$  component dominates. The ratio of the mean square vibrational amplitudes of the surface atoms for Ag(110) to those for Ag(111) at  $0.85T_m$  is around 41, 30, and 5 for the  $x$ ,  $y$ , and  $z$  components, respectively. In order to obtain a qualitative picture of the behavior of the surface atoms for the (111) and (110) (Refs. 37 and 4) surfaces for all three metals, in Fig. 6 we plot the  $z$  component of the mean square vibrational amplitudes because it is the one usually recorded in experimental studies. We find that the vibrational amplitudes for each surface is small up to  $0.5T_m$ , beyond which it enhances the most for Ag(110) which also roughens at about 930 K.<sup>10</sup> The ratio of the  $z$  component of mean square vibrational amplitudes of the surface atoms for (110) to (111) of Ag, Cu, and Ni at a temperature around  $0.63T_m$  are 2, 1.5, and 1 respectively—a trend similar to what Stairis *et al.*<sup>11</sup> noted in their MEIS experiments.

From Table IV and Ref. 16 we conclude that the surface mean square vibrational amplitudes increase at a rate of 18

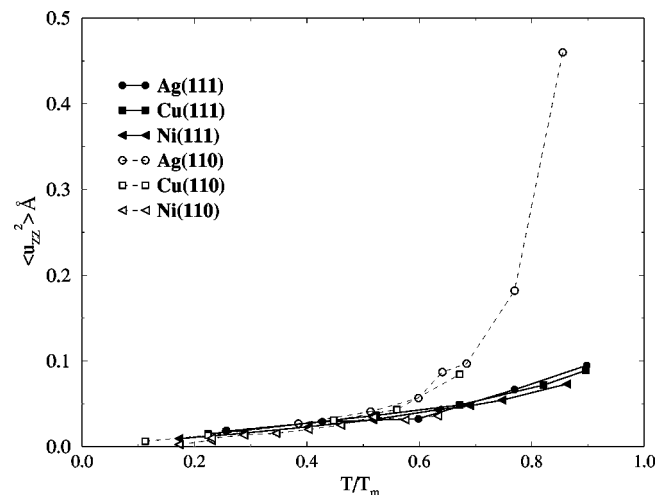


FIG. 6. The  $z$  component of the mean square vibrational amplitudes surface atoms vs the temperature of (111) and (110) surfaces of Ag, Cu and Ni.

TABLE V. Surface mean square vibrational amplitudes normalized to the bulk value for the three components. The last column is the root mean square vibrational amplitude with error bars of  $\pm 0.05$ .

Element	$T(K)$	$\frac{\langle u_x^2 \rangle}{\langle u_B^2 \rangle}$	$\frac{\langle u_y^2 \rangle}{\langle u_B^2 \rangle}$	$\frac{\langle u_z^2 \rangle}{\langle u_B^2 \rangle}$	$\frac{\langle u_{S_{rms}} \rangle}{\langle u_{B_{rms}} \rangle}$
Ag(111)	300	1.42	1.40	1.76	1.24
	500	1.48	1.34	1.64	1.22
	700	1.47	1.44	1.78	1.25
	900	1.41	1.47	1.81	1.26
	1000	1.70	1.57	2.21	1.35
	1050	1.82	1.69	2.1	1.37
	1100	2.33	1.88	2	1.44
Cu(111)	300	1.34	1.31	1.86	1.23
	700	1.37	1.41	1.87	1.25
	900	1.47	1.41	1.80	1.26
	1100	1.50	1.56	1.83	1.28
	1200	1.60	1.61	1.97	1.31
Ni(111)	300	1.33	1.40	2.00	1.26
	500	1.34	1.39	2.03	1.26
	700	1.40	1.40	2.06	1.28
	900	1.41	1.42	2.01	1.27
	1100	1.43	1.45	2.06	1.28
	1200	1.47	1.56	2.07	1.30
	1300	1.54	1.52	2.09	1.31
1500	1.65	1.58	2.11	1.33	

$\times 10^{-5}$ ,  $15 \times 10^{-5}$ ,  $9 \times 10^{-5}$ , and  $7 \times 10^{-5}$   $\text{\AA}^2/\text{K}$  from room temperature up to  $0.5T_m$ , for Ag(111), Cu(111), Ni(111), and Al(111),<sup>16</sup> respectively. From  $0.5T_m$  up to  $0.86T_m$  [for Al(111) up to  $0.80T_m$ ], the rates of the increase of the mean square vibrational amplitudes are  $34 \times 10^{-5}$ ,  $20 \times 10^{-5}$ ,  $18 \times 10^{-5}$ , and  $8 \times 10^{-5}$   $\text{\AA}^2/\text{K}$  for Ag(111), Cu(111), Ni(111), and Al(111),<sup>16</sup> respectively. These rates by themselves would indicate that anharmonic effects on Ag(111) are stronger than those on the other three metals. To examine if this is indeed the case, in Table V we have put together the temperature variation of the ratio of the components of the mean square vibrational amplitudes of the surface atoms to those of the bulk, for the three metals. We find this ratio to be larger in the direction normal to the surface than in the in-plane directions, in agreement with previous theoretical work.<sup>4,38-40</sup> Furthermore, the surface root mean square (rms) vibrational amplitude is almost uniformly larger than that in the bulk by about 30%, for all cases. In the case of the atoms in second and third layers, the rms amplitudes are, respectively, about 18% and 12% larger than that in the bulk. In the entire temperature range considered in the Table, the variation is only 8%, 7% and 6% for Ag(111), Cu(111), and Ni(111), respectively. The anharmonicity on Ag(111) is thus found to be no different than on the other two surfaces.

In Fig. 7 we compare the calculated ratios of the surface to bulk vibrational amplitude with those reported from ex-

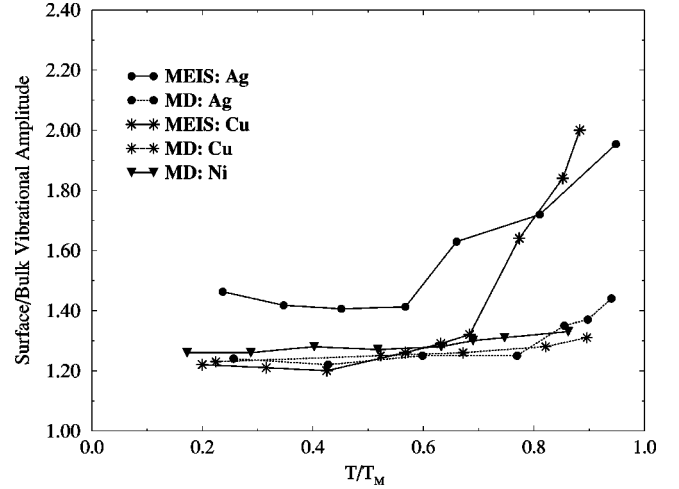


FIG. 7. Ratio of surface-to-bulk vibrational amplitudes versus normalized temperature of Ag(111) and Cu(111): comparison of results from (present work) and MEIS (Refs. 11 and 12). Also included are the MD results for Ni(111).

perimental data for Ag(111) and Cu(111).<sup>11,12</sup> We find good agreement between the calculated and the experimental values for Cu(111) to almost  $0.7T_m$ , after which the measurements show a large increase, reaching a value of 2 close to  $T_m$ . For Ag(111) the calculated values lie below those from MEIS data over the entire temperature range, the discrepancy being much larger beyond  $0.6T_m$ . The figure also includes our results for Ni(111). The MEIS measurements for Ni(111) (Ref. 13) found that up to 1100 K the surface vibrational amplitude is about 30–40% larger than that for the bulk, in good agreement with our calculation. To our knowledge, no measurements are available above 1100 K for Ni(111).

The temperature variation of the mean square vibrational amplitudes is a good indicator of the strength of anharmonic effects. Since for a harmonic system this variation is linear with temperature, the slope of  $\langle u_{i\alpha}^2 \rangle / T$  plotted against  $T$ , as shown in Fig. 8, provides an estimate of the extent of anharmonicity. We see that on each surface anharmonicity sets in

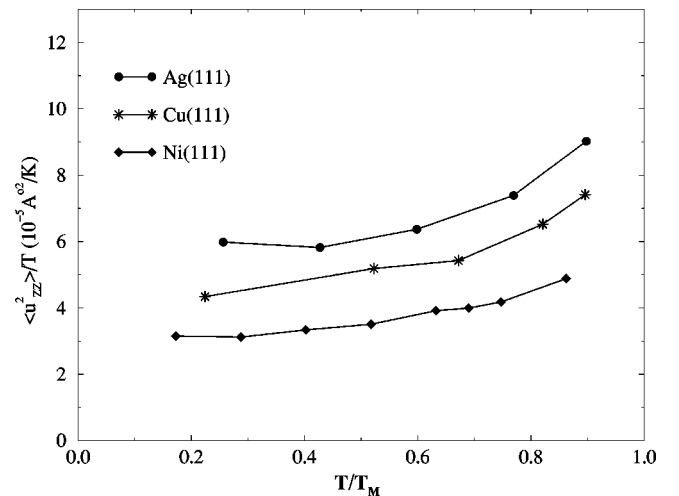


FIG. 8. A plot of  $\langle u_{i\alpha}^2 \rangle / T$  vs temperature for a measure of surface anharmonicity.

TABLE VI. Debye temperature for Ag(111), Cu(111), and Ni(111): the first column represent the bulk value while the second columns represent the surface Debye temperature.

Element	$\theta_B$ (K)	$\theta_S$ (K)
Ag(111)	186.00	143
Cu(111)	237.42	216
Ni(111)	384.10	303

at a particular temperature. Of course, proper accounting of the deviation from harmonic behavior requires inclusion of error bars in the calculation. A comparison with a similar figure for Ag(110) (Fig. 5 of Ref. 37) shows that the anharmonicity on Ag(111) is smaller than that on Ag(110).

The practical implications of the deviations of the mean square vibrational amplitudes are, of course, reflected most in the Debye Waller factors [ $2W(j) \approx (\mathbf{K} \cdot \mathbf{u}_j)^2$ , where  $\mathbf{K}$  is the momentum transfer of the incident particle] which account for the temperature dependence of the scattering intensity from solids. These factors are calculated easily from Table IV. As expected from the discussion above, the Debye-Waller factors approach bulk values as one moves from the top atomic layers to the layers below: the attenuation (to bulk values) happens faster for Ni(111) than the other two surfaces.

### C. Debye temperature

The surface and bulk mean square vibrational amplitudes presented in the previous section can be used to determine another useful quantity called the Debye temperature, defined by

$$\theta_{B(S)}^2 = \frac{9\hbar^2 T}{Mk_B \langle u_{B(S)}^2 \rangle}, \quad (3)$$

where  $M$  is the mass. Our calculated values of the surface and bulk Debye temperature for Ag(111), Cu(111) and Ni(111) are summarized in Table VI. As expected the surface Debye temperatures are smaller than the ones for the bulk due to the enhanced vibrational amplitudes which are the consequence of reduced coordination. We find here  $\theta_S = (3/4)\theta_B$  to be compared with  $\theta_S = (2/3)\theta_B$  for Pd(110).<sup>41,42</sup>

### D. Interlayer separation

The interlayer separation at each temperature is obtained from the time averaged position of each atom in the layer, which is further averaged over the atoms in the layers. In the statistics, we do not include atoms that either diffuse or evaporate away from a layer. The number of such atoms is always small (less than 10% at high temperatures for the top layer and almost negligible for the second and subsequent layers). We define  $\Delta d_{12}$  as  $(d_{12} - d_B)$  where  $d_{12}$  is the average distance between the first and the second layer. The surface percentage relaxations  $\Delta d_{12}/d_B\%$  are plotted in Fig. 9, as a function of temperature. We see that at low temperatures there is a contraction on all three metal surfaces, with Ag(111) relaxed the most followed by Cu(111). As the tem-

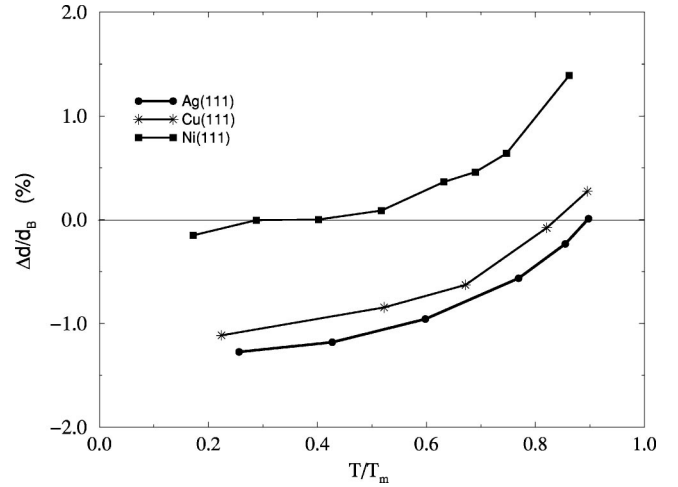


FIG. 9. Percentage change of  $d_{12}$  relative to bulk versus normalized temperature for Ag(111), Cu(111), and Ni(111).

perature increases from room temperature up to  $0.89T_m$ , the surface interlayer spacing for Ag(111) barely reaches the bulk value. For Cu(111) a small enhancement over the bulk value is found above  $0.84T_m$ , and for Ni(111) the surface interlayer spacing overtakes that in the bulk at  $0.40T_m$  and reaches an enhancement of 1.4% at  $0.85T_m$ . Similar calculations show no contraction on Al(111),<sup>16</sup> as  $d_{12}$  is found to remain almost constant up to  $0.8T_m$ , while the bulk expands as the temperature increases.

A comparison of our results for  $\Delta d_{12}/d_B\%$  with the analysis of the experimental data obtained by medium energy ion scattering<sup>11-13</sup> shows that our results are in good agreement up to around  $0.5T_m$  for all three metals; above this temperature our calculations show smaller thermal expansion for all surfaces as compared to that obtained from the MEIS data which find 10% for Ag(111) and 5% for Cu(111) at the high temperature end of the plot. Interestingly, for Ni(111), our calculation and the MEIS data<sup>13</sup> show full agreement up to  $0.64T_m$ . Recent experiments using x-ray diffraction<sup>43</sup> for the case of Ag(111) is in full agreement with our predictions.

### E. Anharmonic constant and Grüneisen parameter

From the previous results, the temperature dependent shifts in the frequencies of the surface phonons and the surface thermal expansion, we calculate two constants that provide a measure of surface anharmonicity: the anharmonic constant and the Grüneisen parameter. The anharmonic shift of surface phonon energies with temperature is generally assumed,<sup>19</sup> in a first approximation, to be proportional to the harmonic energy of the corresponding oscillator, as for molecular vibrations,

$$\hbar\omega(T) = \hbar\omega_0 - \mathcal{X}_e \hbar\omega_0 (2n_0 + 1), \quad (4)$$

where  $w_0$  is the harmonic phonon frequency,  $n_0 = [\exp(\hbar\omega_0/kT) - 1]^{-1}$  is its temperature-dependent occupation number, and  $\mathcal{X}_e$  is the so-called anharmonic constant which will be deduced below for the three surfaces of interest. In a previous theoretical work<sup>18</sup> the above equation was

TABLE VII. The anharmonic constant for Ag(111), Cu(111), and Ni(111) at  $\bar{M}$ .

Element	L	SV
Ag(111)	0.024	0.036
Cu(111)	0.014	0.021
Ni(111)	0.024	0.021

used to produce values for  $\mathcal{X}_e$  ranging from 0.0144 to 0.0183 for Cu(110), using frequencies of the  $S_1$ ,  $S_2$ ,  $S_3$  and  $S_5$  modes at the  $\bar{Y}$  point in the surface Brillouin zone as obtained from MD simulations.<sup>7</sup> The anharmonic constant for Al(111) was similarly calculated to be 0.0203 (using the measured frequencies at different temperatures<sup>44</sup> yielded a value of 0.0240). By applying the same procedure, we present in Table VII. the values of  $\mathcal{X}_e$  for the longitudinal and shear vertical modes for Ag(111), Cu(111) and Ni(111) at  $\bar{M}$ . Our results show that  $\mathcal{X}_e$  range between 0.014 and 0.036 for the three surfaces. The calculated values of  $\mathcal{X}_e$  for Cu(110), Al(111), Ag(111), Cu(111), and Ni(111) are thus found to be similar and small, indicating that anharmonic effects for these surfaces are small.

In order to relate the shift in the frequencies of the surface phonons to surface thermal expansion, we calculate the Grüneisen parameter, which is defined as

$$\gamma_p = - \frac{\Delta \omega_p / \omega_p}{\Delta V / V}. \quad (5)$$

Here  $\gamma_p$  is the Grüneisen parameter for mode  $p$  of frequency  $\omega_p$  and  $V$  is the volume of the crystal. For present purposes, we take  $V = A \cdot d_{12}$ , where  $A$  is the area of the surface. Plots of  $\Delta \omega_p / \omega_p$ , as a function of  $\Delta V / V$  at the high symmetry point  $\bar{M}$  in the surface Brillouin zone for the two modes up to  $0.86T_m$  are shown in Figs. 10 and 11. The surface Grüneisen parameter for the longitudinal and shear vertical modes

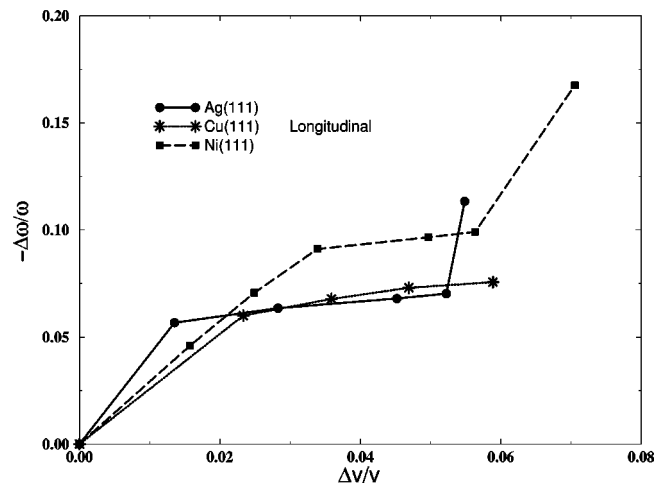


FIG. 10. Variation of the change in longitudinal phonon frequency at  $\bar{M}$  with the change in the volume of the top two layers to determine the Grüneisen constant for Ag(111) and Cu(111) and Ni(111).

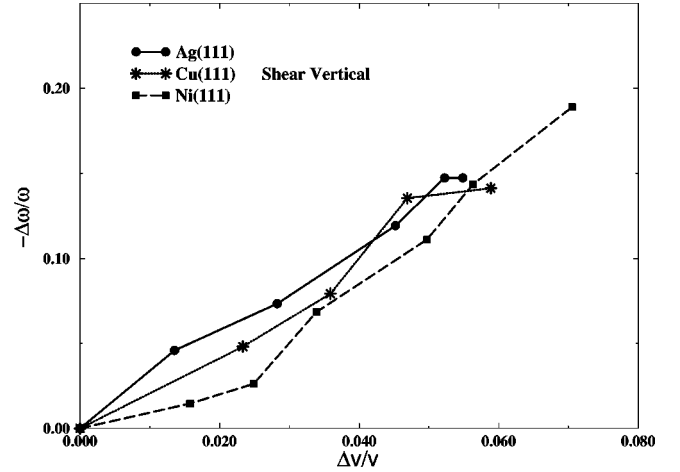


FIG. 11. Variation of the change in shear vertical phonon frequency at  $\bar{M}$  with the change in the volume of the top two layers to determine the Grüneisen constant for Ag(111) and Cu(111) and Ni(111).

from the linear fit of our data for the (111) surfaces of Ag, Cu, and Ni and the results for the bulk from a previous work<sup>45</sup> are given in Table VIII. We are not aware of any previously reported values of  $\gamma$  for (111) surfaces with which we can compare.

### F. Layer order parameters

Snap shots of the top three layers of Ag(111), Cu(111), and Ni(111) from MD simulations show that the three systems have well defined layers for all temperatures even close to melting. To further quantify the disorder on the surface and to examine the possibility of premelting, we present results for two order parameters calculated for the temperature range 300 K to about  $0.9T_m$ . The long-range translational order of the atoms on the surface can be calculated by the static structure factor ( $S$ ) using the relation<sup>46</sup>

$$S(\mathbf{Q}) = \langle |\rho(\mathbf{Q})|^2 \rangle, \quad (6)$$

with

$$\rho(\mathbf{Q}) = \frac{1}{N} \sum_{j=1}^N e^{-i\mathbf{Q} \cdot \mathbf{R}_j}, \quad (7)$$

where  $N$  is the number of atoms in the layer and  $\langle \dots \rangle$  stands for an ensemble average. Here  $\mathbf{Q}$  is the in-plane reciprocal lattice vector  $(2\sqrt{2}\pi/a, 2\sqrt{2}\pi/\sqrt{3}a, 0)$  where  $a$  is the lattice constant. On the other hand, the local order on the

TABLE VIII. The surface Grüneisen parameter for Ag(111), Cu(111), and Ni(111) at  $\bar{M}$ .

Element	Our calculations		Data from previous calculations (Ref. 45)	
	$L$	$SV$	Bulk calculation	Bulk measurement
Ag(111)	1.41	2.66	2.40	2.20
Cu(111)	1.26	2.58	1.96	1.63
Ni(111)	2.01	2.84	1.88	1.90



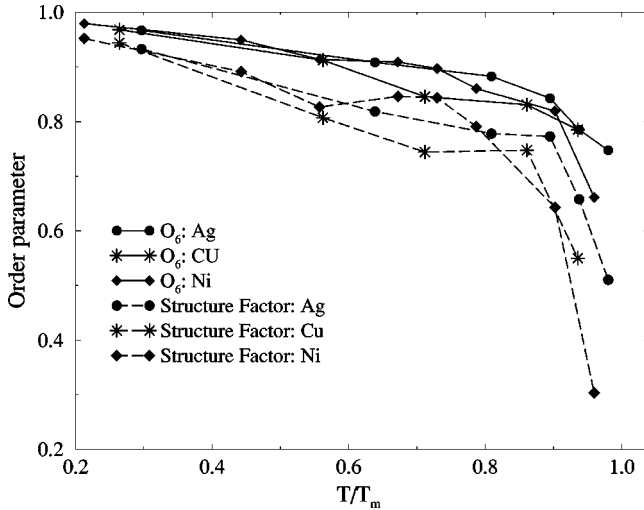


FIG. 12. Top layer order parameters as functions of normalized temperature for Ag(111) and Cu(111) and Ni(111).

(111) surface of an fcc crystal can be measured by the two dimensional order parameter  $O_6$ ,<sup>47,48</sup>

$$O_6 = \frac{|\sum_{i,j} W_{ij} e^{6i\theta_{ij}}|}{\sum_{i,j} W_{ij}}, \quad (8)$$

where the sums run over first- and second-neighbor pairs and  $\theta_{ij}$  is the angle that the  $i-j$  bond, projected onto the  $x-y$  plane, forms with the  $x$  axis. The weighting function  $W_{ij}$  is given by

$$W_{ij} = \exp\left[-\frac{(z_i - z_j)^2}{2\delta^2}\right], \quad (9)$$

with  $\delta$  as one-half the average interlayer spacing. Its purpose is to filter out “noncoplanar” neighbors. A disordering of the surface layer would be signaled by a vanishing structure factor, while a premelting would be shown by  $O_6$  falling rapidly to zero. Our results for the two order parameters,  $O_6$  (solid lines) and  $S$  (dashed lines) are shown in Fig. 12. We see that the decreases in  $O_6$  and in the structure factor, from the value 1 for a perfectly ordered surface, are rather small until  $0.8T_m$ . Beyond  $0.8T_m$ ,  $O_6$  falls to 0.77, 0.78, and 0.66, and the structure factor falls to 0.5, 0.54 and 0.31, for Ag(111), Cu(111) and Ni(111), respectively. We conclude from the analysis of these order parameters that the (111) surfaces of these three metals are well ordered and do not premelt up to a temperature around  $0.9T_m$ .

### III. CONCLUSIONS

Previous studies have shown that with increasing temperatures anharmonic contributions to the interatomic potential become important and manifest themselves by softening of phonon frequencies, broadening of phonon line-widths, thermal expansion, and nonlinear variations of the atomic

vibrational amplitudes. In this work, we have presented a complete analysis of these anharmonic effects on the (111) surfaces of Ag, Cu and Ni. These calculations provide a comparative study for these metals and both a qualitative and quantitative measures of surface anharmonicity. They confirm the presence of anharmonic effects of all types, as characterized in several decades of literature on the subject. However, our calculated variations of the characteristics of the surface phonons with temperature indicate the presence of only small anharmonic effects on (111) surfaces of these metals. The calculated mean square vibrational amplitudes display a small enhancement in the surface anharmonicity over that in the bulk. The vibrational amplitudes are found to be anisotropic such that those of atoms in the top three layers are generally larger along the surface normal than in the surface plane, in agreement with previous theoretical work on Al(111).<sup>16</sup> As expected, the mean square vibrational amplitudes of the atoms in the top layer increase at a higher rate than those of the second and third layers, the average values of these amplitudes normalized to the bulk value are around 30% for Ag(111), Cu(111) and Ni(111). This average ratio decreases to around 18% of the bulk value for the second layer to around 12% of the bulk value for the third layer. From our results, we conclude that both the surface and the bulk exhibit anharmonic effects at temperatures above  $0.5T_m$ .

Our calculated temperature variation of the top interlayer distance ( $d_{12}$ ) shows that, for Ag(111) this value never exceeds that of the bulk, and for Cu(111) only by about 0.3% at  $0.84T_m$ . On the other hand, there is a somewhat larger surface enhancement on Ni(111), reaching about 1.4% at  $0.84T_m$ . Our results for surface thermal expansion are in agreement with the MEIS data for temperatures below  $0.6T_m$  (Refs. 11 and 12) for Ag(111), Cu(111), and Ni(111).<sup>13</sup> It is only at temperatures above  $0.6T_m$  that our results do not reflect the onset of larger surface thermal expansion the MEIS data report for Ag(111) and Cu(111). However, our results are in excellent agreement with recent x-ray measurement on Ag(111) (Ref. 43) and low energy electron diffraction measurement on Cu(111) (Ref. 49) for the higher temperature range.

The present work provides a comprehensive examination and comparison of anharmonic effects on (111) surface of three important metals. It offers qualitative and quantitative measures of the manifestations of surface anharmonicity in the structural and dynamical properties of those surfaces. Furthermore, by comparison it shows that anharmonic effects are larger on the (110) surface than the (111) surface of the respective metal.

### ACKNOWLEDGMENTS

This work was supported in part by the NSF under Grant No. CHE-0205064. We thank P. Micelli, E. Conrad, T. Gustafson, and H. Over for helpful discussions. T.S.R. also thanks the Alexander von Humboldt Foundation for a Forschungspreis and colleagues at the Fritz Haber Institute, Berlin, for their warm hospitality during her sabbatical leave.

- <sup>1</sup>P. R. Watson, M. Van Hove, and K. Hermann, *Atlas of Surface Structures: Volume 1A (1994) Based on the NIST Surface Structure Database (SSD)* **1A** (1994).
- <sup>2</sup>M.V. Hove, *Low Energy Electron Diffraction. Experiments, Theory and Surface Structure Determination* (Springer, Berlin, 1986).
- <sup>3</sup>Y. Cao and E. Conrad, *Phys. Rev. Lett.* **65**, 2808 (1990a).
- <sup>4</sup>Y. Beaudet, L.J. Lewis, and M. Persson, *Phys. Rev. B* **50**, 12 084 (1994).
- <sup>5</sup>R.N. Barnett and U. Landman, *Phys. Rev. B* **44**, 3226 (1991).
- <sup>6</sup>G. Bracco, *Phys. Low-Dimens. Semicond. Struct.* **8**, 1 (1994).
- <sup>7</sup>L. Yang and T.S. Rahman, *Phys. Rev. Lett.* **67**, 2327 (1991).
- <sup>8</sup>H. Hakkinen and M. Manninen, *Phys. Rev. B* **46**, 1725 (1992).
- <sup>9</sup>C. Malo, C.J. Moses, and R. Tatarek, *Surf. Sci.* **287/288**, 871 (1993).
- <sup>10</sup>T.S. Rahman, Z.J. Tian, and J.E. Black, *Surf. Sci.* **374**, 9 (1997).
- <sup>11</sup>P. Statiris, H.C. Lu, and T. Gustafsson, *Phys. Rev. Lett.* **72**, 3574 (1994).
- <sup>12</sup>K.H. Chae, H.C. Lu, and T. Gustafsson, *Phys. Rev. B* **54**, 14 082 (1996).
- <sup>13</sup>H.C. Lu, E.P. Gusev, E. Garfunkel, and T. Gustafsson, *Surf. Sci.* **352/354**, 21 (1996).
- <sup>14</sup>A.N. Al-Rawi, A. Kara, and T.S. Rahman, *Surf. Sci.* **446**, 17 (2000).
- <sup>15</sup>S.M. Foiles, M.I. Baskes, and M.S. Daw, *Phys. Rev. B* **33**, 7983 (1986).
- <sup>16</sup>R. Zivieri, G. Santoro, and V. Bortolani, *Phys. Rev. B* **59**, 15 959 (1999).
- <sup>17</sup>W. Press, S. Teukolsky, W. Vetterling, and B. Flannery, *Numerical Recipes in Fortran* (Cambridge University Press, Cambridge, 1992).
- <sup>18</sup>G. Benedek and J.P. Toennies, *Phys. Rev. B* **46**, 13 643 (1992).
- <sup>19</sup>H. Ibach and D. L. Mills, *Electron Energy Loss Spectroscopy and Surface Vibrations* (Academic, New York, 1982).
- <sup>20</sup>S. Foiles and J.B. Adams, *Phys. Rev. B* **40**, 5909 (1989).
- <sup>21</sup>Y. S. Touloukian, R. K. Kirby, R. E. Taylor, and P. D. Desai, *Thermal Expansion Metallic Elements and Alloys* (Plenum, New York, 1975), Vol. 12.
- <sup>22</sup>J.P. Hansen and M.L. Klein, *Phys. Rev. B* **13**, 878 (1976).
- <sup>23</sup>M. Marchese, G. Jacucci, and M.L. Klein, *Surf. Sci.* **145**, 364 (1984).
- <sup>24</sup>F. Ancilotto, W. Andreoni, A. Selloni, R. Car, and M. Parrinello, *Phys. Rev. Lett.* **65**, 3148 (1990).
- <sup>25</sup>C.Z. Wang, A. Fasolino, and E. Tosatti, *Phys. Rev. B* **37**, 2116 (1988).
- <sup>26</sup>V. Bortolani, A. Franchini, F. Nizzoli, and G. Santoro, *Phys. Rev. Lett.* **52**, 429 (1984).
- <sup>27</sup>G. Armand, *Solid State Commun.* **48**, 261 (1983).
- <sup>28</sup>Y. Chen, S.Y. Tong, K.P. Bohnen, T. Rodach, and K.M. Ho, *Phys. Rev. Lett.* **70**, 603 (1993).
- <sup>29</sup>J. Black and R.F. Wallis, *Phys. Rev. B* **29**, 6972 (1984).
- <sup>30</sup>J. Black, F.C. Shanes and R.F. Wallis, *Surf. Sci.* **133**, 199 (1983).
- <sup>31</sup>J.S. Nelson, M.S. Daw, and E.C. Sowa, *Phys. Rev. B* **40**, 1465 (1989).
- <sup>32</sup>C.S. Jayanthi, H. Bilz, W. Kress, and G. Benedek, *Phys. Rev. Lett.* **59**, 795 (1987).
- <sup>33</sup>S.Y. Tong, Y. Chen, K.P. Bohnen, T. Rodach, and K.M. Ho, *Surf. Rev. Lett.* **1**, 97 (1994).
- <sup>34</sup>H. Ibach and D. Bruchman, *Phys. Rev. Lett.* **44**, 36 (1980).
- <sup>35</sup>R.B. Doak, U. Harten, and J.P. Toennies, *Phys. Rev. Lett.* **51**, 578 (1983).
- <sup>36</sup>H.M. Mohammed, L.L. Kesmodel, B.M. Hall, and D.L. Mills, *Phys. Rev. B* **37**, 2763 (1988).
- <sup>37</sup>T.S. Rahman, *Condensed Matter Theories* (Nova, New York, 1994), Vol. 9.
- <sup>38</sup>R.E. Allen and F.W.D. Wette, *Phys. Rev.* **179**, 873 (1969).
- <sup>39</sup>A.A. Maradudin and A.E. Fein, *Phys. Rev.* **128**, 2589 (1962).
- <sup>40</sup>B.C. Clark, R. Herman, and R.F. Wallis, *Phys. Rev.* **139**, A860 (1965).
- <sup>41</sup>M. Karimi, G. Vidali, and I. Dalins, *Phys. Rev. B* **48**, 8986 (1993).
- <sup>42</sup>F.C. van Delft, *Surf. Sci.* **251/252**, 690 (1991).
- <sup>43</sup>C.E. Botez, W.C. Elliott, and P.F. Miceli, *Phys. Rev. B* **63**, 113404 (2000).
- <sup>44</sup>M. Gester, D. Kleinhesselink, P. Ruggerone, and J.P. Toennies, *Phys. Rev. B* **49**, 5777 (1994).
- <sup>45</sup>C. Kittel, *Introduction to Solid State Physics*, 3rd ed. (Wiley, New York, 1953).
- <sup>46</sup>C.P. Toh, C.K. Ong, and F. Ercolessi, *Phys. Rev. B* **50**, 17 507 (1994).
- <sup>47</sup>P. Carnevail, F. Ercolessi, and E. Tosatti, *Phys. Rev. B* **36**, 6701 (1987).
- <sup>48</sup>K.J. Strandburg, *Rev. Mod. Phys.* **60**, 161 (1988).
- <sup>49</sup>Y. D. Kim, H. Over, A. Al-Rawi, and T.S. Rahman (unpublished).
- <sup>50</sup>J.T. Harten and C. Wöll, *Faraday Discuss. Chem. Soc.* **80**, 137 (1985).
- <sup>51</sup>L. Chen, L. Kesmodel, and J. Kim, *Surf. Sci.* **350**, 215 (1996).
- <sup>52</sup>B.M. Hall, D.L. Mills, H.M. Mohammed, and L.L. Kesmodel, *Phys. Rev. B* **38**, 5856 (1988).